J Mater Sci (2007) 42:6260–6266
DOI 10.1007/s10853-006-1179-0

Study on the damping behavior of Al/SiC$_p$ composite in thermal cycling

Hongxiang Zhang · Mingyuan Gu

Received: 14 April 2006 / Accepted: 25 October 2006 / Published online: 21 April 2007

Abstract A SiC particulate reinforced 1040 commercially pure aluminum was thermally cycled in air between 20 and 300 °C up to 500 cycles. And the damping capacities of the specimens after 50 and 500 cycles were measured against temperature and strain amplitude. Thermal cycling causes the increase in damping, and dislocation damping is the main mechanism. A damping peak was observed in the range of 150–200 °C, which is related to dislocation motion. Thermal cycling leads to the increase in the peak temperature. The activation energy of the internal friction peak was calculated by Arrhenius equation, yielding 1.02 and 1.09 eV for 50 and 500 cycles, respectively. Increase in dislocation during thermal cycling is responsible for the increase in peak temperature and activation energy.

Introduction

Metal matrix composites (MMCs) are generally reinforced with ceramic fibers, whiskers, or particles which have considerable varying chemical and physical properties from the matrix. However, the great difference in coefficient of thermal expansion (CTE) between the matrix and the reinforcement will lead to thermal stresses near the interfaces. During thermal cycling, the accumulation of these thermal stresses around the reinforcements might be high enough to cause the destruction of the material (i.e., thermal fatigue) [1–8].

H. Zhang (✉) · M. Gu
State Key Laboratory of Metal Matrix Composites,
Shanghai Jiao Tong University, No. 1954 Huashan Rd,
Shanghai 200030, China
e-mail: zhanghongxiang@yahoo.com

These stresses can be relieved by two kinds of mechanisms: damage accumulation and microplastic deformation. The first mechanism can take place either by debonding in the matrix/reinforcement interface [1, 2] or by formation and growth of cracks across these interfaces [3], leading to fracture of the reinforcements. The second mechanism is caused by a process of dislocations generation and motion [4, 5]. As for SiC particulate reinforced Al composite, the well-bonding has been observed [6]; an increase in dislocation concentration near the interfaces occurred during the thermal cycling [7, 8].

In recent years damping behavior has been used to represent the microstructure and properties of MMCs. Lavernia et al. discussed main damping mechanisms in MMCs which were related to the microstructural defects [9]. Several studies have shown the contribution of dislocation motion to the overall damping [10]. A damping peak related to the dislocation motion was observed in Al matrix MMC reinforced by alumina fibers [11]. This peak was also observed in Al/SiC$_p$ MMC by Wang [12], and the activation energy of the peak was calculated. This energy is an overall representation of dislocation motion, but its mechanism is very complicated.

The objectives of the present paper are to report thermal stress relaxation performed on Al/SiC$_p$ composite after thermal cycling and discuss the results in connection with the dislocation motion during thermal cycling. The internal friction (IF) technique is very efficient in the study of stress relaxation [13, 14].

Materials and experimental procedure

The materials used for this work are 1040 commercially pure aluminum composites reinforced by 50 vol.% SiC particulates (average sizes 20 μm). All specimens of Al/SiC composites were fabricated using the technique of vacuum pressure infiltration.

Composite materials were annealed at 490 °C for 3 h and then left to cool down in the furnace. Thermal cycling experiments were performed in air between 20 and 300 °C up to 500 cycles. The specimens were heated in the furnace to the desired temperature for 5 min and then cooled down in the water for 1 min. Figure 1 shows the schematic process of thermal cycling.

The composite specimens after 50 and 500 thermal cycles were machined to 35 ×5 ×1 mm^3 by a sectioning machine from Allied High Tech Products Inc. using a diamond wafering blade. By means of dynamic mechanical thermal analyzer (DMA 2980 type), the damping capacities of these specimens were measured between 20 and 300 °C for determining the relationship of internal friction (tan Φ) vs. temperature (*T*) at frequencies of 0.1, 0.5, 1.0 and 4.0 Hz. In addition, the damping and modulus values at room temperature were also measured when the strain amplitude (ε) ranged from 4×10^{-6} to 6×10^{-4} at a constant frequency of 1 Hz.

Experimental results

An optical micrograph of the Al/SiC_p after 500 cycles of heat treatment is shown in Fig. 2. It could be found that, SiC particulates distribute uniformly, and the majority of particulates are in the approximate size of reference value offered by the supplier. Furthermore, the matrix/reinforcement interfaces remain well-bonded.

The curves of internal friction (tan Φ) vs. temperature (*T*) at constant strain amplitude of 1×10^{-4} were plotted in Fig. 3a, b. It is seen from the figures that the damping capacity increases rapidly with increasing temperature and decreasing frequency. And it could be found that a damping peak at the range of 150–200 °C exists in both figures and for every different frequency (as shown by the arrows). The peak tends to higher temperature with the increase in frequencies.

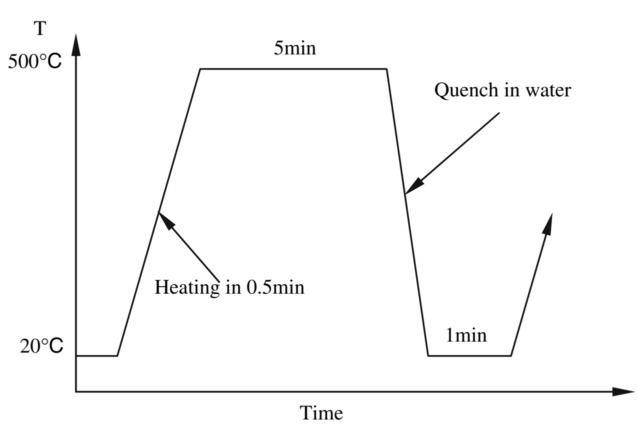

Fig. 1 Schematic process showing one cycle of heat treatment

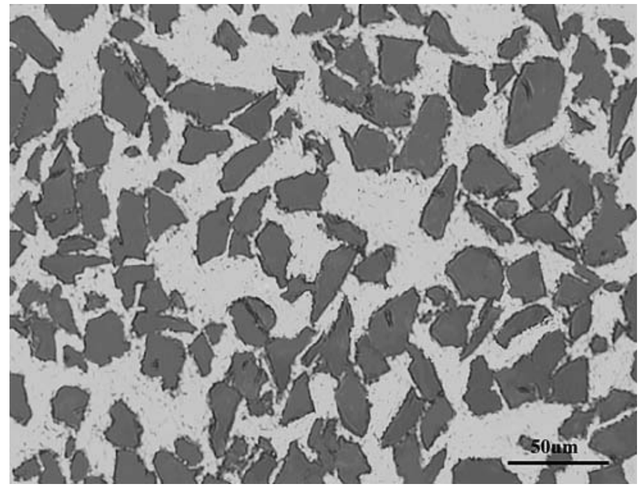

Fig. 2 Optical micrograph of 1040Al/50% SiC_p composite

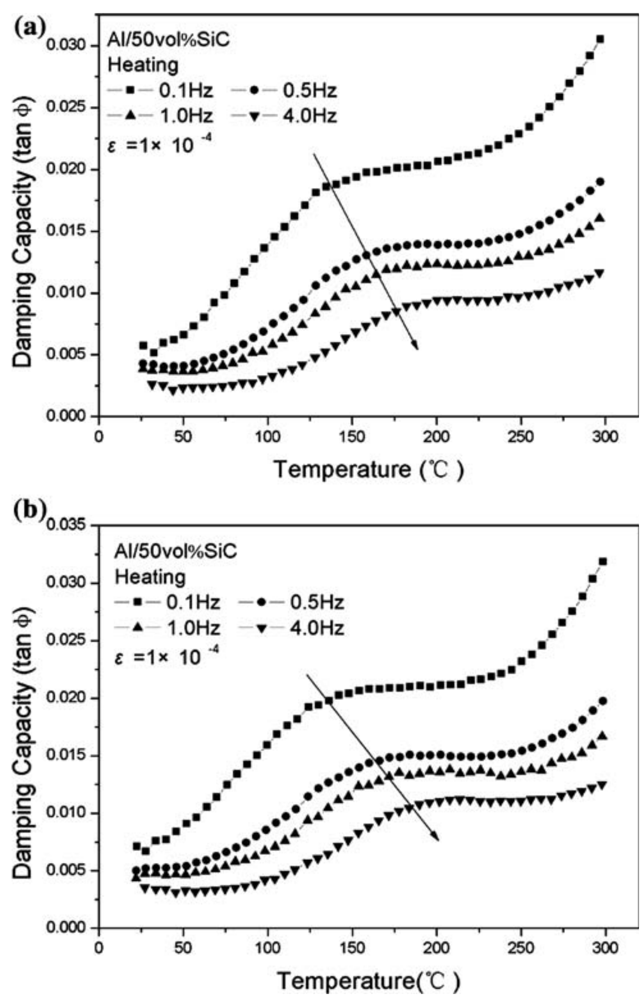

Fig. 3 Internal friction after thermal cycling vs. temperature (**a**) 50 cycles, (**b**) 500 cycles

The dependence of internal friction on strain amplitude ε measured at room temperature and a constant frequency of 1 Hz is depicted in Fig. 4. It can be seen that the damping capacity of Al/SiC$_p$ composite depends on the strain amplitude strongly when the strain amplitude is above 5×10^{-5}.

Discussion

The experiment shows that there exists a damping peak at the range of 150–200 °C (as shown in Fig. 3), whereas it does not exist in aluminum alloy [12]. The absence of the damping peak in Al matrix alloy indicates that the appearance of the peak would be ascribed to the introduction of reinforcements and the microstructural modification to the matrix.

Among the damping mechanisms thermoelastic and microstructural effects (i.e., crystallographic defects) are thought to be the two primary contributors to damping behavior of metallic materials. Thermoelastic damping can be described by irreversible thermal flow produced in metallic materials under mechanical vibration. Defect damping can be ascribed to internal friction acting on reversible intrinsic movement of the microstructural defects in crystalline materials under cyclic loading. The defects include point defects (vacancies and interstitials), line defects (dislocations), surface defects (grain boundaries and interfaces) and bulk defects (micro-pores and micro-cracks). In MMCs, point defect damping is essentially small relative to other sources of defect damping and therefore it can be neglected. In comparison with matrix alloys, the possible dominant damping mechanisms in MMC systems at relatively low temperatures are intrinsic damping of reinforcements, increased dislocation and grain boundary damping in matrix, and matrix/reinforcement interface damping; while at high temperatures, interface slip is likely to be responsible for a large portion of the observed damping [15, 16].

Thermoelestic damping

Thermoelastic damping was originally proposed by Zener [17] based on the fact that energy is dissipated by the irreversible heat flow within a material caused by stress-induced thermal gradients. According to the Zener thermoelasticity theory [17], the thermoelastic damping increases with increasing frequency theoretically as long as the frequencies are less than the Zener relaxation frequency (about 160 Hz for Al MMCs). However, the measured damping for the specimens in the present experiment decreases with increasing frequencies in the whole measuring temperature range. It is therefore proposed that the frequency dependency of the damping for the Al/SiC$_p$ MMCs is not due to thermoelasticity.

Grain boundary damping

Grain boundary damping has been studied in detail by Kê [18] and Zener [17]. The viscous flow at grain boundaries will convert mechanical energy produced under cyclic shear stress into thermal energy, as a result of internal friction at grain boundaries. The thermal energy will then be dissipated through heat exchange with the surroundings. The energy absorbed at grain boundaries is dependent on the magnitude of the shear stress and the grain size. Kê [18] reported that a polycrystalline Al showed higher damping than a single crystal Al when the temperature exceeded 200 °C. In present study, it is shown in Fig. 5 that the difference between the damping of 50 and 500 cycles above 200 °C is relatively small. So it can be proposed that grain boundary damping is not the main mechanism in

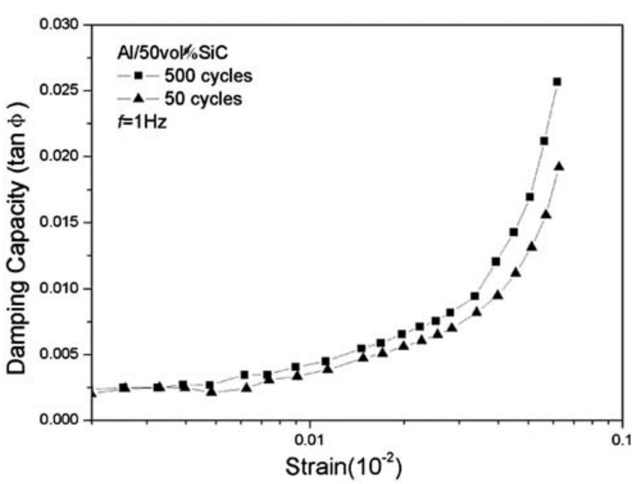

Fig. 4 Damping capacity vs. strain amplitude

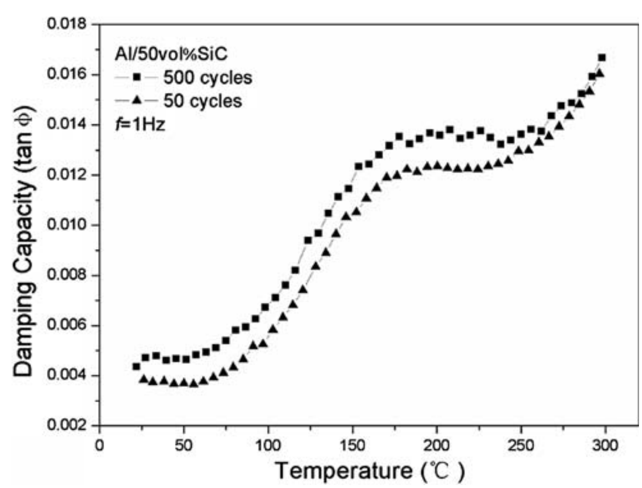

Fig. 5 Internal friction vs. temperature at 1 Hz

thermal cycling. Because of the introduction of reinforcements in the matrix, great thermal mismatch stress led to the thinning of Al grains which may play a partial role in the increase in damping capacity. Thermal cycling can cause the accumulation of residual thermal stresses, and matrix grains will be thinned further. However, this effect is essentially small compared to that from the introduction of high volume fraction of reinforcements. Therefore in thermal cycling, grain boundary damping in MMCs is not the main mechanism.

Interface damping

The interface damping is ascribed to the mobility of the incoherent microstructure at the interfaces and interface slip. In this experiment, interfaces between SiC particulates and Al matrix remained well-bonded through thermal cycling, which was also observed in some studies [6, 19]. While the testing temperature goes up, the metal matrix might become soft relative to the reinforcements and reversible movement at the interface is likely to take place. This effect will lead to the rapid increase in the damping capacity at high temperatures. Therefore the internal friction at the interfaces is thought to be thermally activated, and the interface damping becomes dominant at high temperatures. Schoeck [20] offered a theory to calculate the contribution of the interfaces to damping. Assuming a viscous boundary to exist at the interface at high temperature, the contribution to damping is given by:

$$Q^{-1} \approx [4.5(1-\upsilon)V_{\mathrm{p}}]/[\pi^2(2-\upsilon)], \tag{1}$$

where υ is Poisson's ratio of the matrix, and V_{p} is the volume fraction of the reinforcement. Substitute the values of $\upsilon = 0.33$ and $V_{\mathrm{p}} = 0.5$, yield $Q^{-1} = 0.091$.

At low temperatures, however, the interface damping will not be an important mechanism for the well-bonded interfaces of Al/SiC_p composites.

Considering the intrinsic damping of SiC particulates remains unchangeable, and grain boundary damping is not the main mechanism in thermal cycling; the great change of the damping at low temperatures should be attributed to the matrix dislocations introduced from the residual stress and strain at the interfaces.

Dislocation damping

When the composite is cooled from elevated temperatures of annealing or processing, the metal matrix contracts more than the ceramic particles, and when thermal stresses overcome the matrix flow stress, dislocations move away from the interfaces. In addition, to preserve the continuity between matrix and reinforcement, dislocation loops are punched out from the particles. The increase in the dislocation activity results in an increase in the damping capacity. At low temperatures, there is a hardening of the plastic zones and dislocations become entangled and more efficiently pinned by solute atoms. The result is a decrease in the dislocation mobility and hence in the damping capacity. During subsequent heating, dislocation mobility increases and recombination occurs. Because the matrix expands more than the reinforcements, part of the dislocations generated during cooling are pushed back to the particles. This dislocation dynamics near the interfaces has been evidenced by using in situ TEM [21]. In the case of a pure matrix, the result is the evolution of microplastic zones around the reinforcements, which can grow until distances of the order of the interparticle spacing. And the approximation of the range of the plastic zone has been given by Hill [22].

Considering the MMC as a multiphase system, the damping capacity can be written as the sum of contributions from the reinforcements, the ''normal'' matrix far from the reinforcements and the microplastic zones around the reinforcements, which are denoted with the indexes p, m, zp, respectively:

$$\tan\phi \approx \tan\phi_p + \tan\phi_m + \tan\phi_{zp} = \frac{1}{\pi}\frac{\sum \Delta w_i f_i}{\sigma_0^2/G_{\mathrm{mmc}}}, \tag{2}$$

where Δw_i and f_i are the energy dissipated in a unit volume and the volumetric fraction of the phase i, respectively, G_{mmc} is the elastic shear modulus of the composite and σ_0 the amplitude of the alternative applied shear stress, $\sigma = \sigma_0 \sin(\omega t)$. Neglecting the dissipation inside the reinforcements and in the matrix far from the reinforcements, the main contribution to the damping capacity results:

$$\tan\phi \approx \tan\phi_{zp} = \frac{1}{2\pi}\frac{\Delta W_{zp}}{W} = \frac{f_{zp}\oint \sigma \mathrm{d}\varepsilon}{\pi\sigma_0^2/G_{\mathrm{mmc}}}. \tag{3}$$

Assuming that

$$\mathrm{d}\varepsilon = \dot{\varepsilon}\mathrm{d}t \tag{4}$$

the damping capacity becomes:

$$\begin{aligned} \tan\phi_{zp} &= f_{zp}\frac{\int_{t=0}^{t=2\pi/\omega} \sigma_0 \sin(\omega t)\dot{\varepsilon}\mathrm{d}t}{\pi\sigma_0^2/G_{\mathrm{mmc}}} \\ &= \frac{G f_{zp}}{\omega\pi\sigma_0^2}\int_{\omega t=0}^{\omega t=2\pi} \sigma_0 \sin(\omega t)\dot{\varepsilon}\mathrm{d}(\omega t). \end{aligned} \tag{5}$$

The cyclic applied stress contributes to the dissipation only when it acts in the same direction as the thermal stresses, which means during half of a period:

$$\tan\phi_{zp} = \frac{G_{\mathrm{mmc}} f_{zp}}{\omega\pi\sigma_0^2} \int_{\omega t=0}^{\omega t=\pi} \sigma_0 \sin(\omega t)\dot{\varepsilon}\mathrm{d}(\omega t). \quad (6)$$

From Eq. 6, the damping capacity of the plastic zone is inversely proportional to the frequency ω. Considering the contributions from the reinforcements and the matrix far from the reinforcements are comparatively small, the damping capacity of the composite will decrease with the increasing frequency.

Figure 2 showed that there were no severe damages observed at the interfaces. It is because annihilation or climb of the dislocations during heating might release the strains created from the mismatch in the CTEs and protect interfaces from debonding. Thermal cycling results in the accumulation of the residual strain in the matrix, which can lead to the increase in dislocation concentration in the plastic zone. Therefore, the increase in the overall damping capacity during thermal cycling should be ascribed to the dislocation damping.

According to Granato–Lücke (G–L) theory [23, 24], the dislocation structure is assumed to consist of segments of length L_N along which weak pinning points are distributed randomly, the dislocations are pinned by fine precipitation. At low temperature, dislocation can only drag the weak pinning points (such as some solute atoms, vacancies, etc.) moving and thus dissipating energies, with increasing temperature, the stress for break-away from weak pinning points is decreased because the process is thermally activated [25]. Therefore, when above a certain temperature, dislocation would move faster and then break-away dramatically from the weak pinning point. It would then become a long and comparatively free dislocation in the condition of hard pinning (such as network node of dislocation, the second phase, etc.), the energy dissipated by dislocation motion would not increase, and the damping value may decrease slightly. Consequently, a damping peak is caused. After that, the damping may increase again due to the contribution of interface damping. The phenomenon was obviously shown in Fig. 3a, b. This process is a stress relaxation course. As it is known to all, relaxation strength can be calculated from damping height, and relaxation time τ can be obtained from peak temperatures. These are realized by using Arrhenius equation, which is expressed by [26]

$$\tau = \tau_0 e^{H/kT}, \quad (7)$$

where τ_0 is the inverse attempt frequency, H the activation energy and k the Boltzmann's constant. At the peak temperatures T_{p}, the circle frequency ω is related to the relaxation time τ by $\omega\tau = 1$. Thereby, Eq. 7 can be described by a new expression of the form:

$$\log\omega + \log\tau_0 + \left(\frac{H}{2,303k}\right)\left(\frac{1,000}{T_{\mathrm{p}}}\right) = 0. \quad (8)$$

In light of the data in Fig. 3, the peak temperatures were obtained as shown in Table 1, and the Arrhenius relation was plotted in Fig. 6 from the data in Table 1. Then the activation energy H for specimens after 50 cycles and 500 cycles were calculated being 1.02 and 1.09 eV, respectively. This activation energy is the overall representation of dislocation motion. Comparatively large energy of the sample after 500 cycles indicates that there are more dislocations lying in this sample. Peak temperature (T_{p}) is the reflection of activation energy in the experiment. It can be found from Fig. 5 that, the sample after 500 cycles has a higher peak temperature than that after 50 cycles (the values are shown in Table 1), which indicates the increase in dislocation density during thermal cycling.

Figure 4 reveals the change of damping against strain amplitude after different thermal cycles. Damping of the composite depends on stress and strain. The damping capacity goes up rapidly with the increase in strain amplitude above 5×10^{-6}. The strain amplitude dependence of internal friction suggests the dislocation unpinning processes. G–L theory is used to explain the results. At low applied strain amplitudes, the dislocation segments bow out between the weak pinning points and remain anchored at the strong pinning points. As strain amplitude is increased, the force on the dislocation segments becomes higher than the binding force of the pinning points. So the dislocation segments break away from some points. This leads to an instantaneous increase in dislocations and thus results in the increase in damping.

According to the vibration-string model, the internal friction in low-frequency ranges (kHz), Q^{-1}, is given by [23, 24]

$$Q^{-1} = Q_{\mathrm{a}}^{-1} + Q_{\mathrm{f}}^{-1} \quad (9)$$

$$Q_{\mathrm{a}}^{-1} = \frac{C_1}{\varepsilon}\exp\left(-\frac{C_2}{\varepsilon}\right) \quad (10)$$

Table 1 Values of T_{p} at various frequencies for different cycles

Frequency (Hz)	0.1	0.5	1	4
T_{p} (°C)				
50 cycles	127.10	153.70	167.07	181.93
500 cycles	134.85	162.86	170.47	189.59

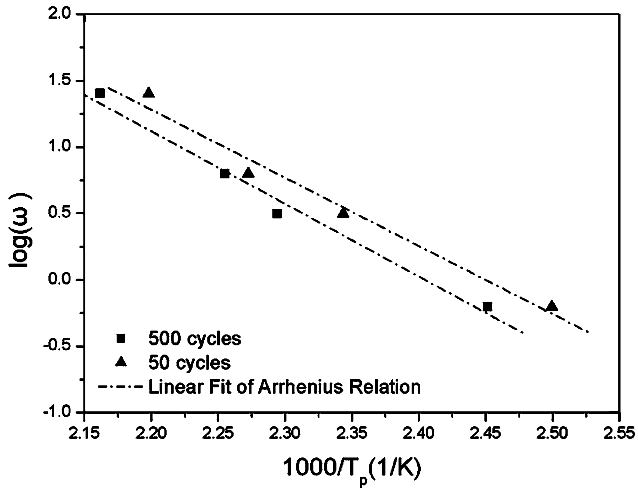

Fig. 6 Arrhenius relation between circular frequency and the peak temperature deduced from the data shown in Fig. 3

$$Q_f^{-1} = \frac{C_3 \rho f^2}{b^2}, \qquad (11)$$

where C_1, C_2 and C_3 are physical constant, ρ the dislocation density, ε and f the vibration strain amplitude and frequency, respectively. At low strain amplitudes, dislocation damping mainly results from the frequency-dependent part, Q_f^{-1}, and beyond a critical strain amplitude, the strain amplitude-dependent, Q_a^{-1}, becomes dominant.

From Eq. 5, another form could be obtained:

$$\ln(\varepsilon Q_a^{-1}) = -C_2 \frac{1}{\varepsilon} + \ln C_1 \qquad (12)$$

which implies that a plot of $\ln(\varepsilon Q_a^{-1})$ vs. $1/\varepsilon$ should yield a straight line. According to the measured data from Fig. 4, the value of $\ln(\varepsilon Q_a^{-1})$ as a function of $1/\varepsilon$ was calculated. The result is shown in Fig. 7. From the figure, it is apparent that the predicted Granato–Lücke linear fit is reasonable, which also indicates that Granato–Lücke theory is effective for the composite in this experiment. Dislocation motion is thought the main course of damping generation at low temperature. Generally, the natural logarithm value of dislocation density is proportional to the intercept of the straight line (i.e.,$\rho \propto C_1$) in Fig. 7 (values of C_1 and C_2 shown in Table 2). It can be shown that the dislocation density in the composite increases largely with thermal cycling.

Figure 7 also shows the difference between two slopes (C_2). The slope of straight line for 500 cycles is slightly larger than that for 50 cycles. According to reference [24], the slope is given by:

$$C_2 = K\varepsilon' b / L_c, \qquad (13)$$

where K is a constant related to the matrix material, ε' is fractional difference in the size of the solute and solvent atoms, b is burger's vector, L_c is the mean distance between weak pinning points. So C_2 is inversely proportional to L_c. L_c is determined by impurities and vacancies. Thermal cycling lowers L_c a little, for impurities in matrix are nearly invariable. Figure 7 shows that the density of vacancy increases a little during thermal cycling.

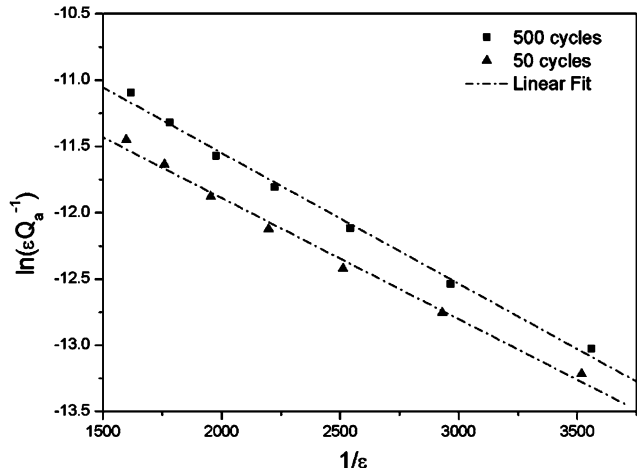

Fig. 7 Granato–Lücke plot of $\ln(\varepsilon Q_a^{-1})$ vs. $1/\varepsilon$ at 1 Hz

Table 2 Calculated values for Eq. 12

	C_1	C_2
50 cycles	4.2808×10^{-5}	9.1471×10^{-4}
500 cycles	6.9368×10^{-5}	9.8638×10^{-4}

Conclusion

Experimental results showed the temperature and strain amplitude dependence of the damping properties of the Al/SiC_p composite after thermal cycling. Based on the analyses of the results in accordance with theories, the following conclusions can be drawn:

1. Thermal cycling causes the increase in internal friction of Al/SiC_p MMC.
2. A damping peak exists at the range of 150–200 °C for all the frequencies studied, and the peak temperature goes up due to thermal cycling. The damping peak is of relaxation model, which is caused by the dislocation motion dragging the weak pinning points under the double action of heat and stress.
3. The activation energy of samples after different cycles was calculated, yielding 1.02 and 1.09 eV for 50 and 500 cycles, respectively. Increase in dislocation during thermal cycling is responsible for the increase in peak temperature and activation energy.

4. Dislocation motion is the main mechanism for the change of the internal fraction of the composite. Increase in dislocation during thermal cycling is responsible for the increase in damping capacity.

Acknowledgement The authors are grateful for the financial supported from Nature Science Foundation of China under Grant No. 50271043.

References

1. Ahn JJ, Ochiai S (2002) J Comp Mater 36:2073
2. Oguocha INA, Radjabi M, Yannacopoulos S (2001) Can Metall Quart 40(2):245
3. Lloyd DJ (1991) Acta Metall Mater 39:59
4. Taya M, Mori T (1987) Acta Metall 35:155
5. Dunand DC, Mortensen A (1991) Acta Metall Mater 39:127
6. Yu D, Chandra T (1995) Mater Sci Forum 189–190:303
7. Trojanova Z, Pahutova M, Kiehn J, Lukac P, Kainer KU (1997) Key Eng Mater 127–131(Pt 2):1001
8. Kustov S, Golyandin S, Sapozhnikov K, Vincent A, Maire E, Lormand G (2001) Mater Sci Eng A 313(1–2):218
9. Lavernia EJ, Zhang J, Perez RJ (1995) Key Eng Mater 104–107:691
10. Parrini L, Schaller R (1996) Acta Mater 44(10):3895
11. Urreta S, Schaller R (1993) Scr Metall Mater 29:165
12. Wang C, Zhu Z (1998) Scr Mater 38(12):1739
13. Parrini L, Schaller R (1995) Metall Trans A 26:1457
14. Vicent A, Lormand G, Durieux S, Girard C, Maire E, Fougeres R (1996) J Phys IV C8:719
15. Zhang J, Perez RJ, Lavernia EJ (1994) Acta Metall Mater 42:395
16. Perez RJ, Zhang J, Gungor RJ (1993) Metall Trans A 24:701
17. Zener C (1948) Elasticity and anelasticity of metals. University of Chicago, Chicago, IL
18. Kê TS (1947) Phys Rev 72:41
19. Flom Y, Arsenault RJ (1986) Mater Sci Eng A 77:191
20. Schoek G (1969) Phys Status Solid 32:651
21. Vogelsang M, Arsenault RJ, Fisher RM (1986) Metall Trans A 17:379
22. Hill R (1983) The mathematical theory of plasticity. Oxford University Press, Oxford
23. Granato AV, Lücke K (1956) J Appl Phys 27:583
24. Granato AV, Lücke K (1956) J Appl Phys 27:789
25. Granato AV, Lücke K (1981) J Appl Phys 52:7136
26. Nowick AS, Berry BS (1972) Anelastic relaxation in crystalline solids. Academic Press, New York